

Surface Microstructure of MMA-HEMA Polymer Membranes

J. M. DOMÍNGUEZ,^{1,*} J. PALACIOS,² G. ESPINOSA,¹ and I. SCHIFTER¹

¹Instituto Mexicano del Petróleo, Subdirección Investigación Aplicada, P.O. Box 14-805, 07730 México D.F.;

²Facultad de Química, UNAM, P.O. Box 20-325, México D.F.

SYNOPSIS

A series of MMA-HEMA polymer (hydroxyethyl methacrylate) membranes were prepared using several copolymer precursor mixtures and were characterized by transmission and scanning electron microscopy. The correlation between the preparation methods and the microstructure of the porous layers was sought. The cryofracture procedures also were investigated in order to observe the polymer membranes in the electron microscope. It was found that the porosity of the intermediate transport layer depends on the molecular weight composition and the MMA/HEMA copolymer ratio; the presence of dimethylformamide (DMF) also has a marked influence on the microtextural properties of the transport layer. The main features of the selective layer surface are the very fine roughness, with pits and pores in the 1–5 nm range, and the chainlike protuberances at the nanometer scale. The cryogenic fracture methods proved adequate for observation of the new MMA-HEMA-type membranes without artifacts. © 1993 John Wiley & Sons, Inc.

INTRODUCTION

Synthetic polymer membranes have been the subject of intensive research recently because of their potential applications in a number of key separation processes.^{1,2} In the search for a correlation between preparation methods and membrane microstructure, a combination of techniques is necessary to obtain the most critical parameters, i.e., the thickness and pore-size distribution of the skin layer,³ the mean pore diameter and pore-size distribution of the transport layer, hydrodynamic resistance (thickness of the top layer), and other properties that determine the permeation properties. Those are important parameters in applications of synthetic polymer membranes in several gas-phase separation processes. Among the more useful methods of characterization of membranes, the adsorption/desorption methods,⁴ the pure water flux and/or gas permeability⁵ selective permeation,⁶ and electron microscopy methods⁷ are the most prominent.

However, the fine microstructure of the skin-layer surface of the gas separation membranes makes it difficult to characterize it unambiguously. In this respect, electron microscopy techniques may give direct information on the pore structure at the sub-nanometer scale, but a careful preparation of the sample is necessary in order to avoid artifacts. In this work, the Pt/carbon replica together with cryofracture methods were investigated and a correlation between the membrane microstructure and preparation parameters was sought. The series of new methyl methacrylate-hydroxyethyl methacrylate (MMA-HEMA)-type membranes were prepared from distinct copolymer precursor mixtures and their physicochemical properties were characterized by several techniques, including NMR, calorimetry, GPC, viscometry, and transmission and scanning electron microscopy.

EXPERIMENTAL

The basic polymers were prepared using reactants including MMA and HEMA monomers, which were extensively purified before use at 59°C/200 mmHg and 67°C/3 mmHg, respectively. The initiators were

* To whom correspondence should be addressed.

Table I Polymer Composition and Their Physicochemical Properties

Sample	MMA (mol %)	N_{THF} (cc/g)	S_g	T_g (°C)	M_n (10^{-4}) g/mol	M_w (10^{-4}) g/mol	DI
MS14	91.0	1.944	1.277	59.0	2.86	5.68	1.98
MS16	82.6	2.6945	1.2656	59.2	3.20	5.33	1.66
MS18	82.7	4.2913	1.2960	61.5	11.74	22.23	1.89
MS22	86.1	3.2698	1.2707	58.7	7.66	17.97	2.30

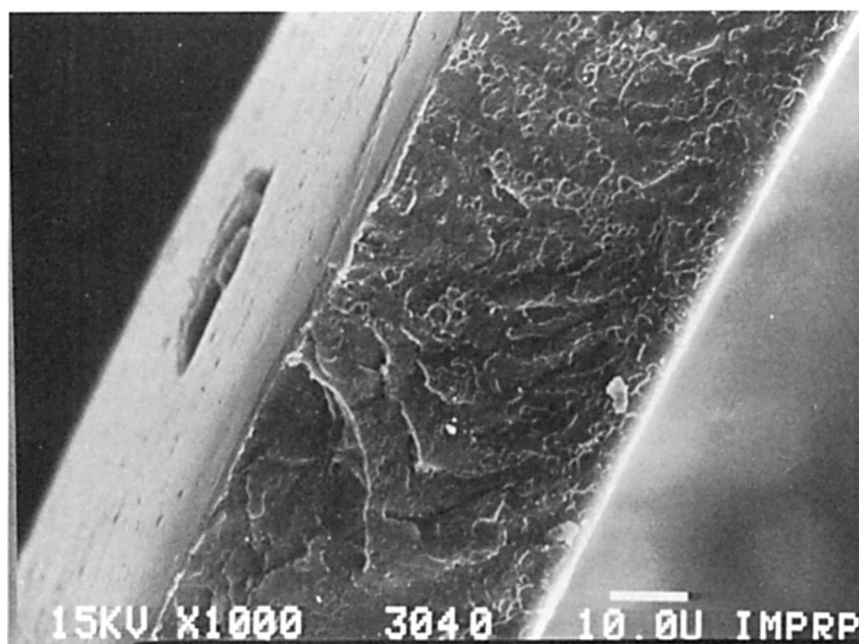
Table II Composition of Precursor Mixtures Used for Membrane Preparation

Polymer (% wt)	MS14A	MS14B	MS16A	MS16B	MS18	MS22
MS14	25	25				
MS16			25	25		
MS18					25	
MS22						25
Chloroform	69	51	69	51	51	51
Butanone	6	6	6	6	6	6
DMF		18		18	18	18

2,2-azobisisobutyronitrile (AIBN) and 2,2-azobis-methylbutyronitrile (AMBN), both compounds of 99.9% of purity. The bulk polymerization of MMA and HEMA was carried out in 5 mL vials in the absence of oxygen using a vacuum treatment (i.e., 10^{-4} Torr); then the vials were kept at a temperature below 0°C. Afterward, the activation of the monomer

mixture was accomplished using microwave radiation, as described previously.⁸

The physicochemical characterization of the copolymers was determined using the simultaneous application of proton magnetic resonance, calorimetry, permeation chromatography, and viscometry. The NMR studies were performed in a Varian

**Figure 1** SEM of the transport layer interface of the MS14A membrane.

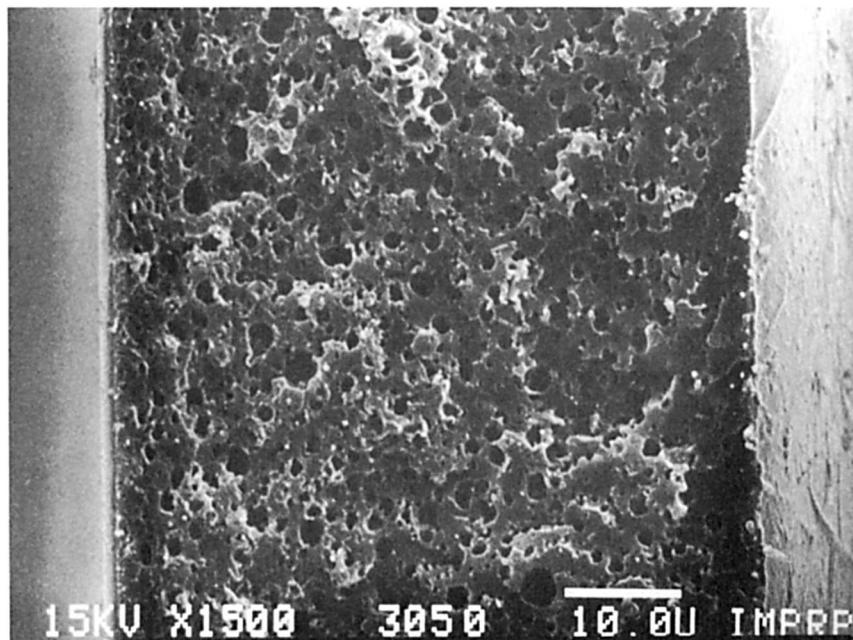


Figure 2 SEM of the transport layer interface of the MS14B membrane.

Em'390 (90 Mhz) spectrometer, using a solvent of deuterated chloroform (CDCl_3), at 30°C . From these data, the real copolymer composition was determined, in mol %.

The thermal studies leading to the determination of heat capacity and the glass transition temperature (T_g) were done using a DuPont-990 instrument, in a sealed pan, at a heating rate of $10^\circ\text{C}/\text{min}$. The

operation mode was consistent with the ASTM D-3918-82 procedure.

The molecular weights and their distribution were determined by gel permeation chromatography (GPC), using a Waters ALC-GPC instrument. The dilute solutions of the polymers (in THF) were characterized at room temperature by two linear columns (Ultra Styragel), which covered a range

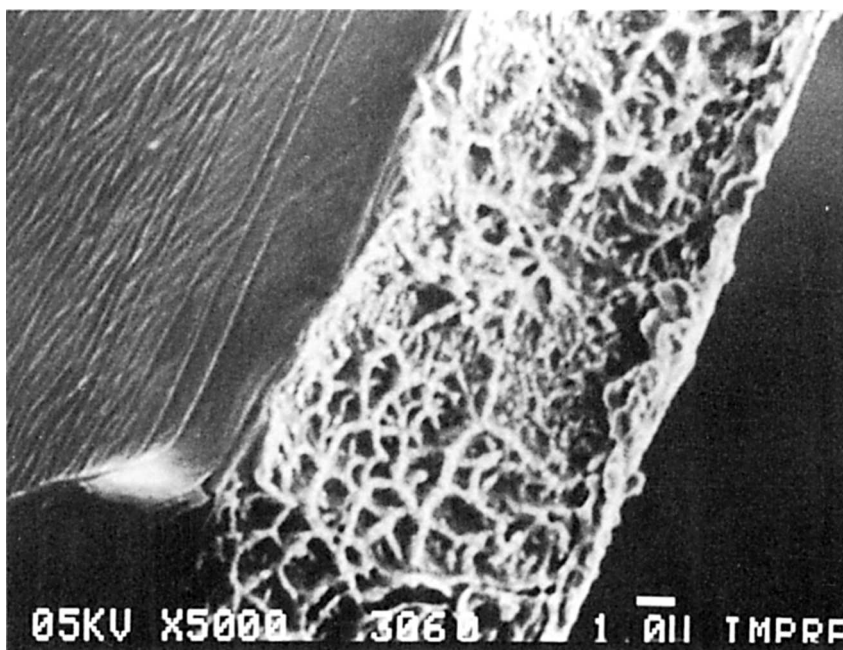


Figure 3 SEM of the transport layer interface of the MS16A membrane.

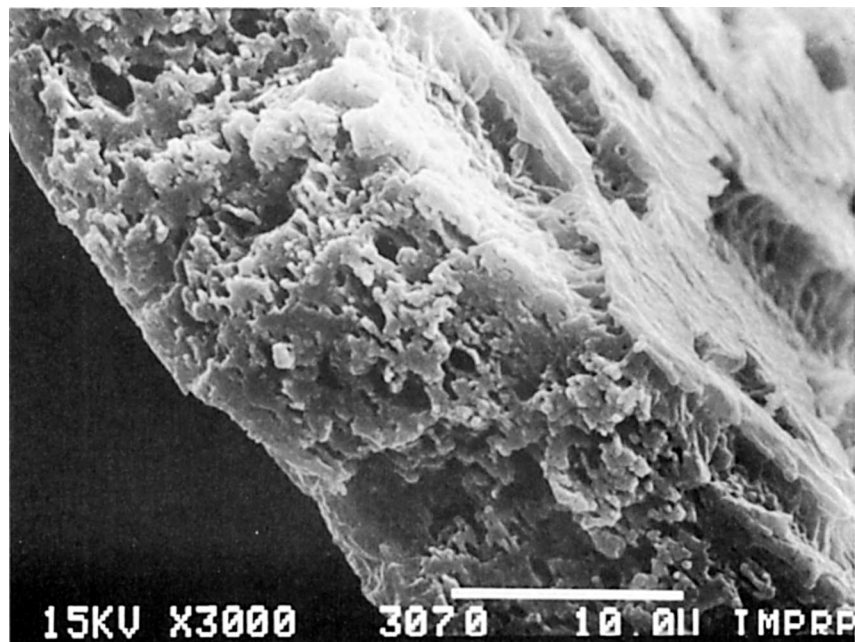


Figure 4 SEM of the transport layer interface of the MS16B membrane.

between 2×10^3 to 4×10^6 g/mol, at a flow rate of 1 mL min^{-1} . The operation was consistent with the ASTM D-2837-70 procedure, which leads to determination of molecular weights \bar{M}_n and \bar{M}_w , as well as with the polydispersity index.

Finally, the reduced and intrinsic viscosities were measured by a Cannon-Fenske instrument at 30°C , following the ASTM D-729-66 procedure. The sol-

vent of choice was THF (good solvent). The specific gravity, as determined by the displacement technique, was determined in water at 25°C .

The physical characterization of the membrane's porosity was determined by a scanning and transmission electron microscope, Jeol-35CF and Jeol-2000 respectively. A series of cross-sectional cuts were obtained by fracture of the samples in liquid

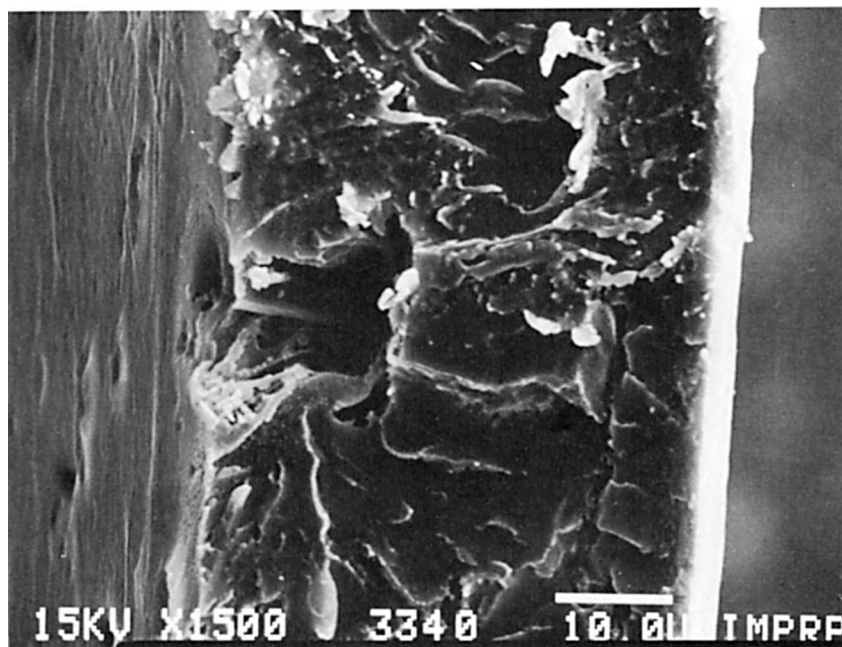


Figure 5 SEM of the transport layer interface of the MS18 membrane.

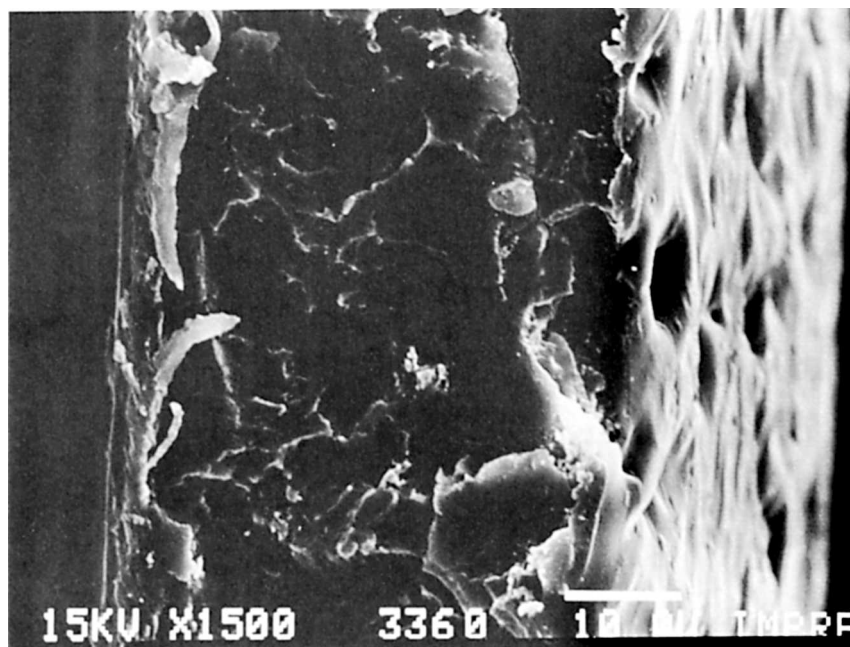


Figure 6 SEM of the transport layer interface of the MS22 membrane.

nitrogen. Then, a coating with chromium metal was applied to enhance the surface contrast. This method allowed the characterization of pores in the transport layer. The skin-layer porosity was investigated by transmission microscopy, but the application of this technique required a careful preparation of the membrane samples, by cryofracture, which was performed in a special chamber that was

cooled adiabatically at a rate of $2 \times 10^5 \text{ }^\circ\text{C s}^{-1}$ to avoid the formation of ice crystals that might lead to artifacts. This method keeps the morphological and structural features to be observed without perturbations that are common in organic films, such as pore contraction due to water loss. The apparatus used was a Balzer EVM 052 fitted with an attachment for deposition of thin Pt/C films of about 0.5-

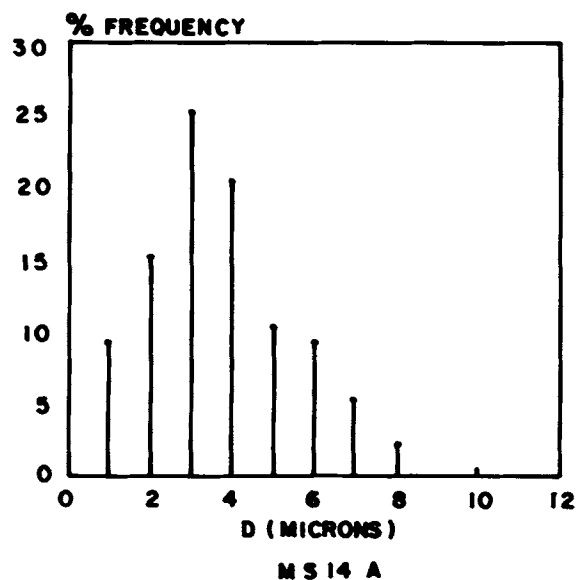


Figure 7 Histogram with pore-size distribution of the transport layer of membrane MS14A.

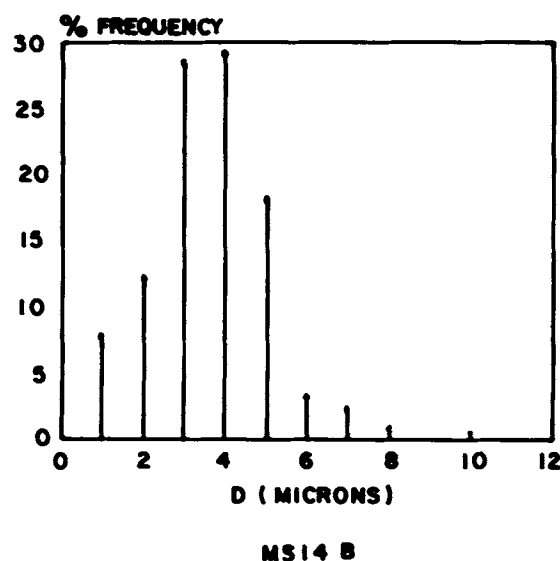


Figure 8 Histogram with pore-size distribution of the transport layer of membrane MS14B.

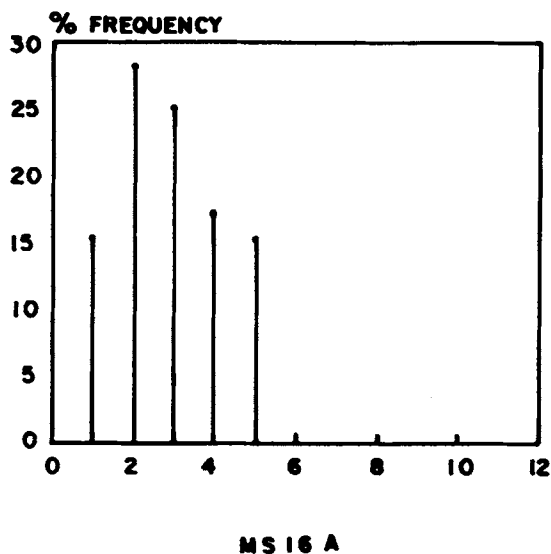


Figure 9 Histogram with pore-size distribution of the transport layer of membrane MS16A.

2 nm thickness. Afterward, these films were floated and mounted onto 200 mesh copper grids.

RESULTS

The experimental data corresponding to the copolymer mixtures are collected in Table I, where the distinct composition of the polymer mixtures is reported (i.e., % mol of MMA) together with the parameters such as the average molecular weights, \bar{M}_n and \bar{M}_w ; the polydispersion index, (DI); the glass transition temperature, T_g ; specific gravity, S_g ; and the dilute solution viscosity, N_{THF} .

Starting with those copolymer compositions, a series of membranes were cast by using the dry method,⁸ but also others were prepared by the wet method using methanol in the precipitation stage. The composition in the former method included dimethylformamide (DMF) in the solvent mixture, with a boiling point of 153°C, which is above the boiling point of butanone and chloroform.

The composition of the precursor mixtures used for casting of the polymer membranes is summarized in Table II. As an example, the membrane MS14B was made from a mixture of 25% wt of MS14 polymer, 51% wt of chloroform, 6% wt butanone, and 18% wt DMF.

The micrographs shown in Figures 1 and 2 correspond to the cross-sectional views of membranes MS14A and MS14B, respectively (see Table I). The main difference in their preparation was the pres-

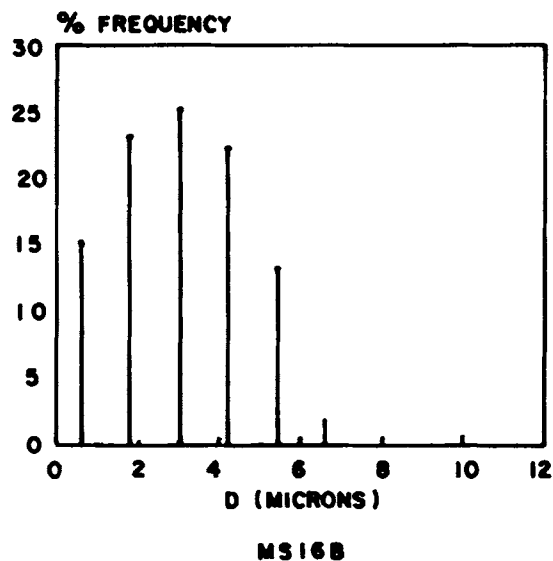


Figure 10 Histogram with pore-size distribution of the transport layer of membrane MS16B.

ence of DMF in the precursor mixture. In both cases, the presence of a skin layer of about 0.9 μm thickness and the increase of porosity due to the DMF content is apparent. This trend is confirmed by the series MS16A and MS16B membranes, shown in Figures 3 and 4, which were prepared with and without DMF, respectively (see Table II). However, the series of membranes that were cast from similar compositions, as e.g., MS18 and MS22, did not adopt the sponge-type microtexture (Figs. 5 and 6).

The pore-size distribution of the intermediate

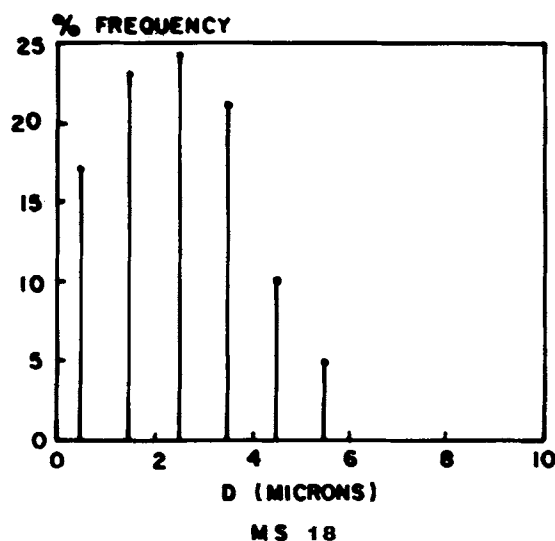
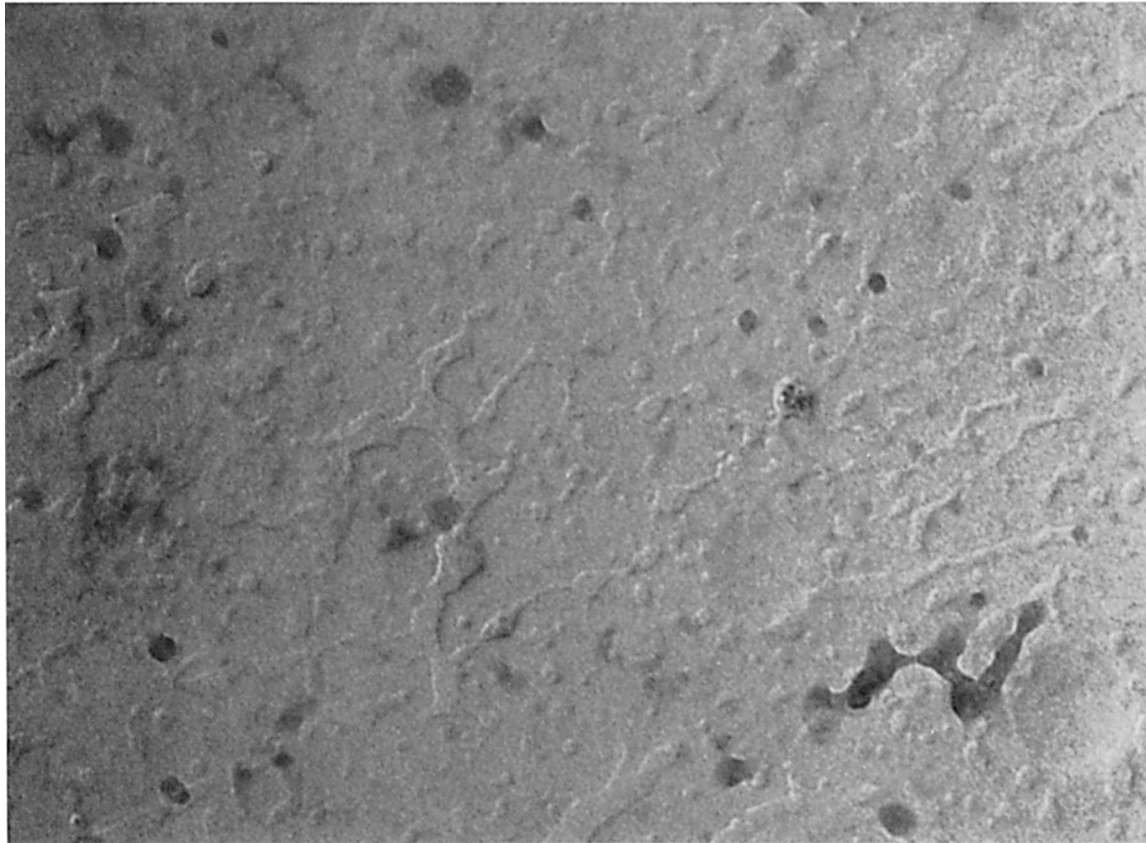


Figure 11 Histogram with pore-size distribution of the transport layer of membrane MS18.



(a)

6nm



(b)

4 nm

Figure 12 (a) Typical high-resolution image of the selective layer face (membrane MS14B). (b) Enlarged view of (a).

transport layer of the membranes was determined from the statistical counting of pore diameters from the scanning micrographs; these results are displayed in Figures 7–11 for the series of membranes. Although the mean pore size oscillates around 3 μm for the whole series, the total pore volume differs in each case, as shown in the histograms.

From Table II it is apparent that the precursor mixture composition of membranes MS16B and MS18 is about the same, the only difference being the polymer molecular weights \bar{M}_n and \bar{M}_w (Table I), which lead to a distinct porosity of the transport layer interface (Figs. 4 and 5), i.e., a higher molecular weight leads to a less porous layer. Similarly, MS14A and MS16A membranes (see Table II) have about the same molecular weight (Table I) but a distinct content in MMA monomer; then, the microtexture difference observed from micrographs (1) and (3) might be attributed to this variation, i.e., a more open structure is obtained when the content of HEMA increases.

Finally, the platinum–carbon replica samples that were cast on the larger faces of membranes were observed in a transmission mode in the electron microscope. A fine structure of the skin-layer surface was observed in all cases, as illustrated here in Figure 12(a), which is a high magnification (i.e., 250 K \times) image corresponding to MS14B membrane. As observed, pits and pores are apparent, plus a fine roughness formed by elongated chainlike protuberances. Figure 12(b) shows an enlarged view of the same field.

In conclusion, surface microstructure and preparative variables of MMA–HEMA-based membranes were investigated and a correlation was sought. It was found that the porosity of the transport layer interface depends on the precursor solvent

mixture composition, i.e., the DMF, and it is inversely related to the molecular weights. The cryogenic fracture methods have been proved adequate for characterization of the synthetic membranes by electron microscopy techniques, thus avoiding artifacts that are common to thin organic films. On the other hand, the selective layer surface, i.e., the skin layer, presents a fine roughness with pits and pores in the 1–5 nm range, with additional elongated chainlike protuberances.

Further work is underway to explore the possible mechanisms for gas diffusion in MMA–HEMA-type membranes and the surface microstructure of the selective layer.

REFERENCES

1. S. A. Stern, in *Synthetic Membranes*, Symposium Series, Ed. M. B. Chenoweth, MMI Press, Washington, DC, 1984, Vol. 5, pp. 1–38.
2. W. A. Bollinger, D. L. MacLean, and R. S. Narayan, *Chem. Eng. Progr.*, **78**(10), 27 (1982).
3. C. Lemoyne, C. Friedrich, J. L. Halary, C. Noël, and L. Monnerie, *J. Appl. Polym. Sci.*, **25**, 1883–1913 (1980).
4. C. A. Smolders and E. Vugteveen, in *Materials Science of Synthetic Membranes*, D. Lloyd, Ed., American Chemical Society, Washington, DC, 1985.
5. T. Matsuura, Y. Taketani, and S. Sourirajan, *J. Colloid Interface Sci.*, **95**, 10–22 (1983).
6. B. A. Farnand, F. D. F. Talbot, T. Matsuura, and S. Sourirajan, *Ind. Eng. Chem. Proc. Des. Dev.*, **22**, 179–187 (1983).
7. W. Pusch and A. Walch, *Angew. Chem. Int. Ed. Engl.*, **21**, 660–685 (1982).
8. J. Palacios, J. Sierra, and M. P. Rodríguez, to appear.

Received May 5, 1992

Accepted September 9, 1992